Journal of The Korean Astronomical Society
37: 471 ∼ 476, 2004

POSSIBLE MERGER SIGNATURE IN SZ MAPS

Patrick Koch
Institute of Astronomy and Astrophysics, Academia Sinica, P.O. Box 23-141, Taipei 106, Taiwan, R.O.C.
E-mail: pmkoch@asiaa.sinica.edu.tw

ABSTRACT

We propose an analytical model to estimate the influence of a merger on the thermal SZ effect. Following observations we distinguish between subsonic and transonic mergers. Using analytical velocity fields and the Bernoulli equation we calculate the excess pressure around a moving subcluster for an incompressible subsonic gas. Positive excess around the stagnation point and negative excess on the side of the subcluster lead to characteristic signatures in the SZ map, of the order of 10% compared to the unperturbed signal. For a transonic merger we calculate the change in the thermal spectral SZ function, resulting from bow shock accelerated electrons. The merger shock compression factor determines the power law tail of the new non-thermal electron population and is directly related to a shift in the crossover frequency. This shift is typically a few percent towards higher frequencies.

Key words : cluster of galaxies – merger – SZ effect

I. INTRODUCTION

Clusters of galaxies generally form by gravitational mergers of smaller clusters and groups. XMM-Newton and Chandra observations reveal detailed structures of merging processes in clusters of galaxies. Moving cold fronts could be identified as the remnants of a subcluster and they are believed to mark the late stage of a merging process (Markevitch *et al.* (1999), Markevitch *et al.* (2000), Vikhlinin *et al.* (2001)). Fewer examples show an early stage merger where the cold core of the subcluster is still surrounded by warmer gas which is not yet fully stripped off. (See e.g. Kempner *et al.* (2002).) Dynamics, geometry and extension of the subclusters can be very different: Whereas the bullet-like southern subcluster in A85 (Kempner *et al.* (2002)) has a radius of curvature of only $19\,kpc$ and is moving with a Mach number $\mathcal{M} \approx \infty.\triangle$ relative to the cluster gas, the cold front in A3667 (Vikhlinin *et al.* (2001)) has a spherical head with a radius of $\approx 410\,kpc$ at $\mathcal{M} \approx \infty.\prime \pm \prime.\in$. A subsonic merger in the very last stage was discovered in RXJ1720.1+2638 (Mazzotta *et al.* (2001)) with $\mathcal{M} \approx \prime.\triangle$. Whereas RXJ1720.1+2638 seems to become fully relaxed, the cold front in A2034 (Kempner & Sarazin (2003)) is being disrupted by gas dynamics instabilities and the region is far from being in hydrostatic equilibrium. Similarly, the merger in A2142 (Markevitch *et al.* (2000)) could only be marginally detected due to its interaction with a possible cooling flow.

For a subcluster moving with $\mathcal{M} > \infty$ a bow shock is expected. A first clear detection was made in 1EO657-56 (Markevitch *et al.* (2001)) with a shock compression factor between the postshock and the preshock region of 3.2 ± 0.8 and a temperature jump from $\approx 8\,keV$ to $\approx 18\,keV$, which corresponds to $\mathcal{M} \approx \in -\ni$. In some cases (e.g. Vikhlinin *et al.* (2001), Allen *et al.* (2002)) there is also evidence for shock heated regions at a temperature much higher than the ambient cluster temperature. As found from simulations (see e.g Ricker & Sarazin (2001), Randall *et al.* (2002)), this is indeed expected to occur if two subclusters collide and the gas in between is compressed. This region is also an important source of non-thermal cluster physics like relativistic particles and magnetic fields.

Based on these observations, we analyze how merging processes might influence the Sunyaev-Zeldovich (SZ) effect. In an earlier work, Komatsu *et al.* (2000) reported an enhanced SZ signal for RXJ1347-1145 at $150\,GHz$. In order to estimate the change in the SZ signal, we calculate the modified pressure profile due to the presence of a merger and, if existing, we take into account non-thermal effects. Our model is based on current X-ray observations and therefore provides a direct comparison between the expected SZ signal and surface brightness for merger events. For this purpose we treat the subcluster as a solid body. Obviously, this scenario has its limitations: Our model is more suitable for late stage merger cold fronts when the surrounding gas is stripped off and the denser core remains. We assume the intracluster gas is spread around the subcluster and smoothly redistributed maintaining a β-model shape. Furthermore, we exclude major mergers and limit the description to merger events where the dark matter distribution in the main cluster and its overall shape are not significantly changed.

Finally, we remark that the SZ effect directly probes the electron pressure and, therefore, is more sensitive to higher temperature regions and pressure jumps than X-ray observations. Furthermore, there is no band limitation as the SZ effect integrates over all the electron population and no redshift dimming. This makes it

Proceedings of The 3rd Korean Astrophysics Workshop on *Cosmic Rays and Magnetic Fields in Large Scale Structure*

a particularly interesting tool for high z clusters with future high spatial resolution.

II. INCOMPRESSIBLE FLOW APPROXIMATION FOR SUBSONIC MERGER

For low Mach numbers in the range of $\mathcal{M} \approx \text{ı.}\triangle - \text{ı.}\forall$, the effects due to compressibility are small. When the fluid is locally compressed, the surrounding plasma tends to spread around quickly, which happens at the speed of sound. With this approximation the fluid dynamics around a reasonably shaped subcluster can be handled analytically. However, we point out that observations of subsonically moving mergers indeed exist. In the following two subsections we first introduce our model for a line of sight and then apply it to construct a SZ merger map.

(a) Model

We assume a merger going through the cluster center and we fix the merger axis parallel to the line of sight. The pressure integration along a line of sight through the cluster center is divided into three regions: the region ahead of the subcluster, the subcluster itself and the region behind. Ahead, an excess pressure contribution due to the movement of the body - in top of the hydrostatic pressure - is expected. Based on the velocity potential for a uniform stationary stream around a body of characteristic shape, the velocity field can be fully determined. Using this result in the Bernoulli equation yields the pressure profile. For the subcluster itself we adopt data from observations. The region behind the subcluster might be turbulent and is not yet well understood. We simply adopt a β-model for the intracluster gas, as it is also done for X-ray observations.

The SZ effect, which is the frequency dependent intensity change of the CMB photon field $\Delta I(x)$ after integration along the line of sight over the cluster (cl) dimension, can be expressed as follows (see e.g. Sunyaev & Zeldovich (1972), Rephaeli (1995)):

$$\Delta I(x) = i_0\, g(x) \int_{cl} \left(\frac{kT_{e,cl}}{m_e c^2}\right) \sigma_T n_{cl}\, dl_{cl}, \qquad (1)$$

where $x = \frac{h\nu}{kT}$ is the dimensionless frequency with T the CMB temperature and $i_0 = \frac{2(kT)^3}{(hc)^2}$. The integral is the Comptonization parameter y describing the cluster properties with $T_{e,cl}$, m_e the electron cluster temperature and mass, respectively. n_{cl} is the electron number density in the cluster and σ_T the Thomson cross section. (k, h, c are the Boltzmann constant, the Planck constant and the speed of light, respectively.) The function $g(x)$ defines the spectral shape of the thermal SZ effect where, for the plasma in clusters, we have $T_{e,cl} \gg T$:

$$g(x) = \frac{x^4 \exp x}{(\exp x - 1)^2} \left(\frac{x(\exp x + 1)}{\exp x - 1} - 4\right). \qquad (2)$$

We define $\Delta SZ_M = \frac{\Delta I_M(x)}{\Delta I(x)}$ as the ratio of the modified SZ signal due to the presence of a merger compared to the unperturbed thermal effect. We assume that the spectral shape for $\Delta I_M(x)$ is in a first order given by $g(x)$ and the ratio ΔSZ_M is thus frequency independent. Possible non-thermal effects are discussed in Section III. ΔSZ_M can thus symbolically be written with the explicit contributions of the three subregions:

$$\Delta SZ_M = \frac{\int_{r_l}^{r_{M,1}} P_<(r)\, dr + \int_{r_{M,1}}^{r_{M,2}} P_M(r)\, dr + \int_{r_{M,2}}^{r_l} P_>(r)\, dr}{2\int_0^{r_l} P_{cl}(r)\, dr}, \qquad (3)$$

where $P_<$ and $P_>$ denote the pressure ahead of and behind the subcluster, respectively. P_M is the pressure inside the merging subcluster which is limited by the two coordinates $r_{M,1}$ and $r_{M,2}$, which can be anywhere on the line going through the cluster center. See Fig.1.

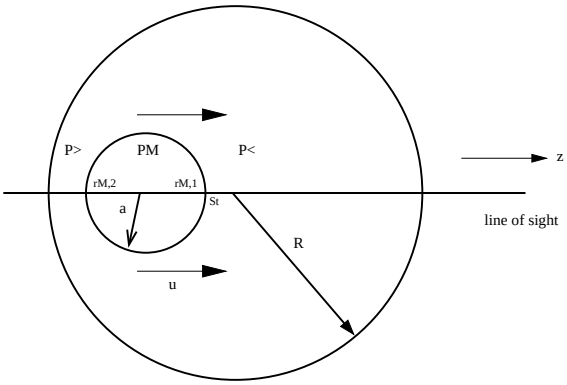

Fig. 1.— A spherical merging subcluster. $r_{M,1}$ and $r_{M,2}$ denote the boundaries of the subcluster moving towards the cluster center with the stagnation point St. The different regions are labeled $P_<$, P_M and $P_>$ .u is the subcluster velocity with respect to the cluster rest frame.

Neglecting the gravitational potential, we find $P_<$ from the Bernoulli equation for a general stationary flow (See e.g. Landau & Lifshitz (1959)):

$$h(r) + \frac{1}{2}v^2(r) = const., \qquad (4)$$

where h is the specific enthalpy and the constant can be evaluated anywhere along a streamline. For an incompressible flow, the enthalpy is simply given by $h(r) = \frac{P(r)}{\rho(r)}$, where $\rho(r)$ is the inhomogeneous (incompressible) underlying intracluster gas profile. Evaluating the constant in the free stream region at the cluster boundary, $const. = \frac{P(r_l)}{\rho(r_l)} + \frac{1}{2}u_\infty^2$, where u_∞ is the free

stream velocity, we find for the pressure profile ahead of the body towards the stagnation point:

$$P_<(r) = \rho(r)\left(\frac{P(r_l)}{\rho(r_l)} + \frac{1}{2}(u_\infty^2 - v(z)^2)\right), \quad (5)$$

for a given velocity profile $v(z)$. The coordinate z is measured from the subcluster center and is related to the cluster coordinate r through the subcluster's variable position. We remark that the above derivation for an infinitesimal streamline can easily be generalized for a finite extension of an instrumental beam as the velocity field is analytically known.
Finally, we assume that the subcluster density in the cold core is approximately constant, as it is motivated by observations. The subcluster extension is $2a$. Eq.(3) can thus be rearranged:

$$\Delta SZ_M = 1 + \frac{1}{2\int_0^{r_l} f(r)\,dr} \times \times \left[\int_{r_l}^{r_{M,1}} f(r)\frac{1}{2}\mathcal{M}_\infty^{\in}(\infty - \frac{\sqsubseteq(\ddagger)^{\in}}{\sqcap_\infty^{\in}})\lceil\nabla - \int_{r_{M,1}}^{r_{M,2}} f(r)\,dr + 2a\frac{n_{e,M}T_M}{n_{e,0}T}\right], \quad (6)$$

where we parametrized the free stream velocity u_∞ with the Mach number $\mathcal{M}_\infty$ relative to the ambient cluster gas ($u_\infty^2 = \mathcal{M}_\infty^{\in}\frac{\|\mathcal{T}}{\mu\Updownarrow_\swarrow}$) and $\rho(r) = \rho_{g,0}f(r)$.

The velocity profile and the resulting excess pressure profile towards the stagnation point for a spherical merging subcluster are given by:

$$v(z) = u_\infty\left(1 + \frac{a^3}{z^3}\right), \quad (7)$$

$$P_{ex}(r) \sim f(r)\frac{1}{2}\left[1 - \left(1 + \frac{a^3}{z^3}\right)^2\right]. \quad (8)$$

In the z-coordinate system, the origin of the sphere is set at $z = 0$. The velocity and pressure profiles are calculated for the off distance $z \le -a$, where $z = -a$ denotes the stagnation point. As the excess pressure depends on the underlying hydrostatic pressure given by the cluster gas profile $f(r)$, the above expressions depend also on the location of the subcluster. As an example we plot the excess pressure profile for a subcluster with $a = 100\,kpc$, located with its forefront at the cluster center, $r = r_{M,1} = 0\,kpc$ in Fig.2. Fig.3 shows the dependence on the cluster core radius. For comparison we also plot the profiles for a cylinder and the streamlined Rankine body as possible subcluster shapes. Depending on the parameters, the excess pressure contribution is in the range of a few percents, typically $2 - 10\,\%$.

To study the influence of the subcluster, we assume $\frac{n_{e,M}T_M}{n_{e,0}T} = 2$ as found in Vikhlinin *et al.* (2001), Fig.4

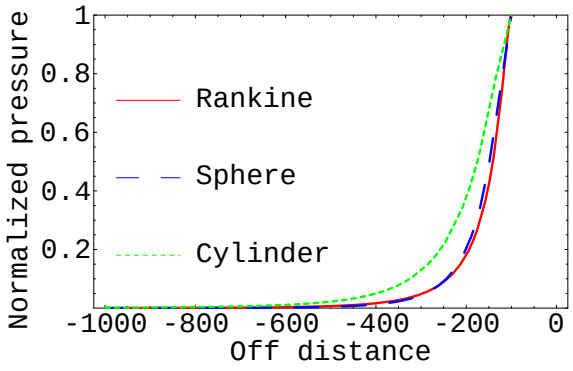

Fig. 2.— Pressure profiles normalized by the stagnation pressure, $a = 100\,kpc$, for the Rankine fairing, the sphere and the cylinder. The stagnation point is at the off distance $-100\,kpc$. The underlying hydrostatic pressure is assumed to be a β-profile with $r_c = 250\,kpc$ and $\beta = 2/3$. The subcluster is located with its forefront at $r_{M,1} = 0\,kpc$.

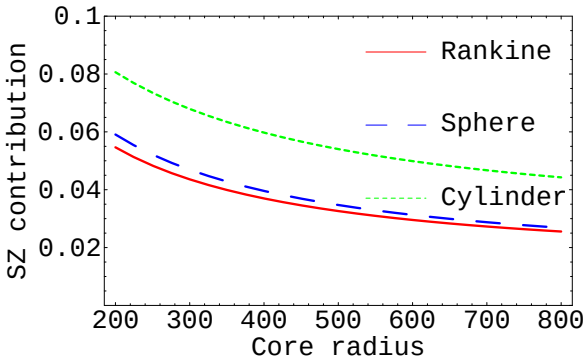

Fig. 3.— The SZ contribution from the excess pressure for $a = 200\,kpc$ as a function of the cluster core radius r_c. The subcluster forefront is at $r_{M,1} = 0\,kpc$, moving at $\mathcal{M}$=0.8.

shows the subcluster contribution as a function of the cluster core radius for different locations. This contribution may give an approximatively 50% additional signal. See also Koch & Jetzer (2004).

(b) Excess Pressure Signature in SZ Maps

Extending the model from the previous section to two dimensions, we can calculate the excess pressure around the merging subcluster from the velocity field $v_r = \frac{\partial\phi}{\partial r}$ and $v_\theta = \frac{1}{r}\frac{\partial\phi}{\partial\theta}$ derived from the sphere velocity potential ϕ:

$$\phi = u_\infty r\cos\theta + \frac{1}{2}a^3 u_\infty\frac{\cos\theta}{r^2}, \quad (9)$$

where the radial coordinate r is measured from the subcluster center and θ is measured in flow direction. Integrating the excess pressure in flow direction leads to a characteristic feature as a result of Bernoulli's equation. As shown in Fig.5, the excess pressure is positive around the stagnation point whereas it is negative on

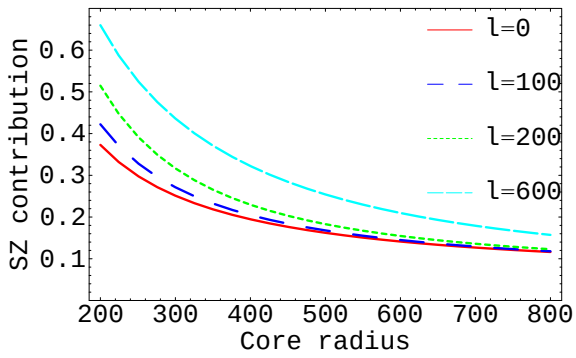

Fig. 4.— The SZ contribution from the subcluster. The cluster core radius is fixed at $r_c = 250\,kpc$. The subcluster extension is $a = 200\,kpc$. The subcluster location is at $r = l = 600, 200, 100, 0\,kpc$ from top to bottom.

the side of the subcluster where the fluid is accelerated. Superimposing the excess pressure with the underlying

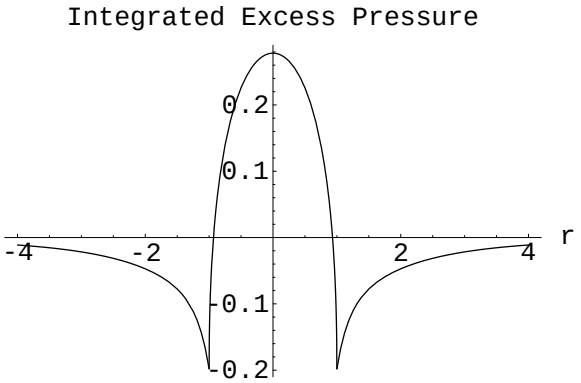

Fig. 5.— Integrated excess pressure along the flow direction in arbitrary units. The radial coordinate r is centered on the stagnation point on the spherical subcluster.

pressure from the β-profile leads to the SZ signal. Fig.6 shows the integrated pressure for a merger parallel to the line of sight, thus integrating the excess pressure along the flow direction. The characteristic knick is caused by the negative excess pressure on the side of the subcluster. A different case, assuming a merger perpendicular to the line of sight, is shown in the map of Fig.7. As it can be clearly seen, the symmetry is broken due to the characteristic feature of the excess pressure. Fig.8 shows a horizontal central cut of Fig.7 and reveals again the negative excess pressure feature. For clarity, the subcluster density is set to the background density of the β-model in all the above figures.

III. TRANSONIC MERGER: NON-THERMAL EFFECTS

In top of the subsonic merger model as described in the previous section, shock waves resulting from transonic mergers are possible energy sources for parti-

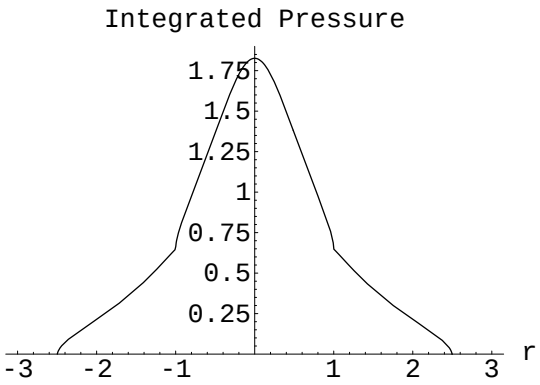

Fig. 6.— Integrated pressure for a merger parallel to the line of sight in arbitrary units.

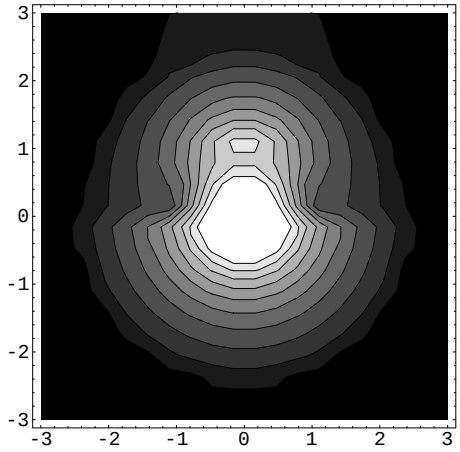

Fig. 7.— Integrated pressure contour map for a merger perpendicular to the line of sight in arbitrary units. Dark color indicates low pressure, bright color indicates high pressure. Clearly seen is the positive excess pressure around the stagnation point and the negative excess on the side.

cle acceleration mechanisms. Relativistic electrons can be accelerated by diffusive Fermi acceleration (Fermi (1949), Blandford & Eichler (1987).) The resulting electron distribution can be described by a Maxwellian with a power law tail. The crucial point is the 'break energy', where the power-law tail replaces the Maxwellian tail. The simulations of Bykov & Uvarov (1999) (see their Fig.2) clearly show that the low energy part of the distribution is less and less well approximated by a Maxwellian, as the 'enhanced' high energy tail extends to lower and lower energies (lower 'break'). Therefore one needs a constraint to define a lower limit for the break energy. Such a constraint has been given by Porquet *et al.* (2001) in the form of $p_1 \geq \alpha + 1/2$ for the below set of equations. For the thermal Maxwellian distribution we choose a relativistic extension:

$$f_{e,th}dp = \frac{\beta_{th}}{K_2(\beta_{th})} p^2 \exp(-\beta_{th}\sqrt{1+p^2})dp, \qquad (10)$$

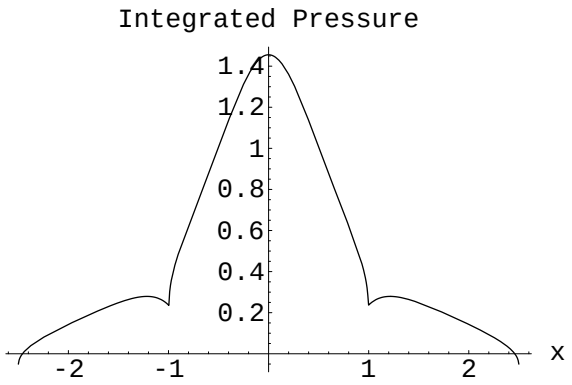

Fig. 8.— Integrated pressure for a merger perpendicular to the line of sight in arbitrary units. Horizontal central cut through Fig.7.

with $\beta_{th} = \frac{m_e c^2}{k_B T_e}$ and $K_2(x)$ the modified Bessel function of the second kind and second order. For the power law tail we write:

$$f_{e,pw} dp = \frac{\beta_{th}}{K_2(\beta_{th})} p_1^2 \exp\left(-\beta_{th}\sqrt{1+p_1^2}\right) \left(\frac{p}{p_1}\right)^{-\alpha} dp, \tag{11}$$

where p_1 is the break energy and the power law index α is related to the shock compression factor $\mathcal{C}$ and the merger Mach number $\mathcal{M}$ by:

$$\alpha = \frac{\mathcal{C} + \in}{\mathcal{C} - \infty} = 2\frac{\mathcal{M}^{\in} + \infty}{\mathcal{M}^{\in} - \infty}. \tag{12}$$

After normalizing the resulting hybrid electron distribution function, we calculate the new spectral function $g(x)$ for the non-thermal SZ effect, adopting the formalism presented by Colafrancesco *et al.* (2002). Similar calculations for different cases have been carried out by Ensslin & Kaiser (2000), Fujita & Sarazin (2001) Gabici & Blasi (2002), Colafranceso *et al.* (2003). Fig.9 shows the change in the spectral function for typical merger parameters. The change in the crossover frequency is of the order of 5%.

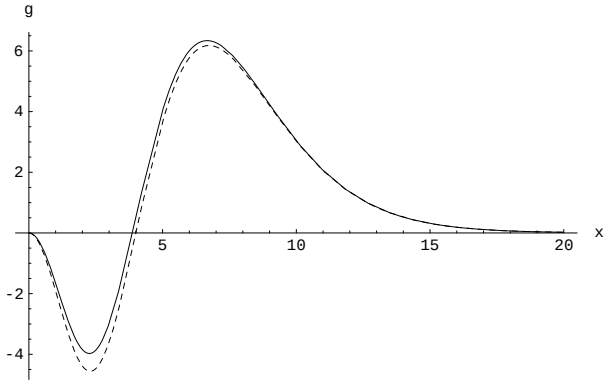

Fig. 9.— Comparison between the spectral functions: The solid line shows the thermal spectral function (Eq.2) and the dashed line is the non-thermal spectral function resulting from a merger event with $\alpha = 3$, $p_1 = 3.5$ and $k_B T_e = 5$.

IV. CONCLUSION

The excess pressure profile resulting from a moving subcluster shows characteristic features which can lead to a distinction between different merger directions. In particular, this can be of interest for subsonic mergers which do not show a bow shock as indication of the merger axis. Moreover, the excess pressure profile should also act as a tracer of compressibility and heating effects. The contribution to the unperturbed SZ signal is of the order of 10%, depending on the exact cluster parameters. The contribution of the subcluster itself can be significant and may even lead to more prominent characteristic features as it basically gives an additive positive component. Transonic mergers will additionally lead to a distortion in the spectral function with a change in the crossover frequency depending on the shock compression.

ACKNOWLEDGEMENTS

The author wishes to thank Dongsu Ryu, Hyesung Kang and all the many helpers for a very stimulating and most enjoyable conference.

REFERENCES

Allen, S. W., Schmidt, R. W., & Fabian, A. C., 2002, astro-ph/0111368

Blandford, R. D., & Eichler, D., 1987, Phys. Rep. 154, 1

Bykov, A. M., & Uvarov, Yu. A., 1999, JETP 88, 465

Colafrancesco, S., Marchegiani, P., & Palladino, E., 2002, astro-ph/0211649

Colafrancesco, S., Dar, A., & De Rújula, A. 2003, astro-ph/0304444

Ensslin, T. A., & Kaiser, C., 200,. AA 360, 417

Fermi, E. 1949, Phys. Rev. 8, 1169

Fujita, Y., & Sarazin, C. L., 2001, astro-ph/0108369

Gabici, S., & Blasi, P., 2002, astro-ph/0207523

Kempner, J. C., Sarazin, C. L., & Ricker, P. M., 2002, astro-ph/0207251

Kempner, J. C., & Sarazin, C. L., 2003, astro-ph/0304310

Koch, P. M., & Jetzer, Ph., 2004 astro-ph/0406461

Komatsu, E., et al. 2000, astro-ph/0006293

Landau, L. D., & Lifshitz, E. M., 1959, in *Fluid mechanics*, Oxford: Pergamon Press

Markevitch, M., Sarazin, C. L., & Vikhlinin, A., 1999, ApJ 521, 526

Markevitch, M., et al. 2000, ApJ 541, 542

Markevitch, M., et al. 2001, astro-ph/0110468

Mazzotta, P., Kaastra, J. S., Paerels, F. B., Ferrigno, C., Colafrancesco, S., Mewe, R., & Forman, W., 2001, astro-ph/0107557

Porquet, D., Arnaud, M., & Decourchelle, A., 2001, AA 373, 1110

Randall, S. W., Sarazin, C. L., & Ricker, P. M., 2002, ApJ 577, 579

Rephaeli, Y., 1999, Annu. Rev. Astron. Astrophys. 33, 541

Ricker, P. M., & Sarazin, C. L., 2001, astro-ph/0107210

Sunyaev, R. A., & Zel'dovich, Ya. B., 1972, Comm. Astrophys. Space Phys. 4, 173

Vikhlinin, A., Markevitch, M., & Murray, S. M., 2001, ApJ. 551, 160